Experimental Diabetic Neuropathy With Spontaneous Recovery

Is There Irreparable Damage?

James M. Kennedy and Douglas W. Zochodne

Progressive diabetic neuropathy has hitherto been irreversible in humans. New approaches raise the question of whether islet cell reconstitution rendering euglycemia can reverse specific features of neuropathy. We evaluated physiological and structural features of experimental neuropathy in a long-term murine model of diabetes induced by streptozotocin. By serendipity, a subset of these diabetic mice spontaneously regained islet function and attained near-euglycemia. Our hypotheses were that this model might better reflect axon loss observed in human disease and that spontaneous recovery from diabetes might identify the features of neuropathy that are reversible. In this model, experimental neuropathy closely modeled that in humans in most critical aspects: declines in motor conduction velocities, attenuation of compound muscle (*M* waves) and nerve action potentials, axon atrophy, myelin thinning, loss of epidermal axons, and loss of sweat gland innervation. Overt sensory neuron loss in dorsal root ganglia was a feature of this model. In mice with recovery, there was robust electrophysiological improvement, less myelin thinning, and remarkable epidermal and sweat gland reinnervation. There was, however, no recovery of populations of lost sensory neurons. Our findings identify a robust model of human diabetic neuropathy and indicate that overt, irretrievable loss of sensory neurons is one of its features, despite collateral reinnervation of target organs. Sensory neurons deserve unique protective strategies irrespective of islet cell reconstitution. *Diabetes* 54:830–837, 2005

Until the early part of the last century, diabetes was a diagnosis that meant certain death within a few years. The discovery of insulin allowed control of the disease but also drew the adverse complications of the disease to the forefront. Elevated prevalence and globalization of the disease, particularly over the past 2 decades (1,2), has strengthened the focus on developing a potential "cure" for it, reinforced recently through the use of islet cell transplantation (3). It remains to be determined, pending control or cure of diabetes, whether the initial adverse effects set in motion by derangements in glycemia are reversible.

Neuropathy is unfortunately a common complication of patients with uncontrolled diabetes (4,5). At the point of clinical detection, significant impairments in nerve function (i.e., distal sensory loss) may have already surfaced and handicapped patients (6). Sensory, motor, and autonomic fibers can all be targeted by chronic hyperglycemia (7), typically occurring in a distal-to-proximal gradient starting in the lower extremities. Loss of light touch and pain are predominant features that can predispose individuals to unrecognized foot lesions, ulcerations, and limb loss secondary to gangrene. Neuropathic pain early and muscle weakness later are additional major burdens. The underlying cause of diabetic polyneuropathy remains controversial. It likely includes a number of mechanisms involving polyol flux, microangiopathy with ischemia, neurotrophin deficiency, excessive protein glycosylation, and heightened oxidative stress leading to structural changes on a genetically susceptible background.

In this work we provide extensive and novel characterization of neuropathy in long-term experimental murine diabetes. The model provided direct parallels with several features of human disease that have thus far eluded rat models. By serendipity, a subset of mice spontaneously regained islet function and recovered from diabetes with near-euglycemia. This feature allowed us to address questions about how reversible neuropathy might be in the setting of β-cell reconstitution, an emerging therapy in human diabetes.

RESEARCH DESIGN AND METHODS

Procedures were approved by the animal care committee of the University of Calgary in accordance with the Canadian Council on Animal Care. Adult male Swiss Wistar mice (20–30 g, $n = 60$; Department of Biosciences, University of Calgary) were housed two per plastic cage (8) on a 12-h light/dark cycle, with food and water available ad libitum. Mice were assigned randomly to either a diabetic or control group, and diabetes was initiated by three consecutive injections of streptozotocin (STZ; 50 mg/ml Zanosar; Upjohn, Don Mills, ON, Canada) in citrate buffer (pH 4.8) during the fasting state (one intraperitoneal injection per day: 85 mg/kg on day 1; 70 mg/kg on day 2; and 55 mg/kg on day 3). Control animals received equivalent volume doses of the citrate buffer solution.

Hyperglycemia was verified 1 week later by sampling from a tail vein. A fasting whole–blood glucose level ≥16 mmol/l (normal 5–8 mmol/l) was our criterion for experimental diabetes. Whole–blood glucose tests were carried out using an Accuchek IIm (Boehringer Mannheim, Dorval, PQ, Canada), whereas plasma glucose was checked with a glucose oxidase method (Ektachem DT-II analyzer; Eastman Kodak, Rochester, NY). The cohort of mice

From the Department of Clinical Neurosciences and the Neuroscience Research Group, University Of Calgary, Calgary, Alberta, Canada.

Address correspondence and reprint requests to Dr. D.W. Zochodne, University of Calgary, 3330 Hospital Dr. NW, Calgary, Alberta T2N 4N1, Canada. E-mail: dzochodn@ucalgary.ca.

Received for publication 9 June 2004 and accepted in revised form 15 November 2004.

STZ, streptozotocin

TABLE 1
Weights and glucose

Group	Weight (g)	Glucose (mmol/l)
Diabetic (n = 5)	34.5 ± 2.1*	31.9 ± 1.5*
Recovered (n = 7)	39.4 ± 1.2*	8.2 ± 0.4†
Nondiabetic (n = 7)	50.4 ± 2.5	6.2 ± 0.2

Data are the means ± SE. Comparisons between groups used a one-way ANOVA with Bonferroni post hoc comparisons. Glucose represents plasma glucose taken at the end of the 9 months. *P < 0.01; †P < 0.05.

TABLE 2
Electrophysiological end points

Group	Motor conduction velocity (m/s)	Sensory conduction velocity (m/s)	M wave potential amplitude	NAP amplitude
Diabetic	24.8 ± 2.9*	35.3 ± 1.3	3.3 ± 0.3*	199 ± 18*
Recovered	50.2 ± 4.7*	36.7 ± 0.8	5.2 ± 0.6	266 ± 14
Nondiabetic	40.1 ± 2.2	39.2 ± 1.4	5.5 ± 0.6	251 ± 9

Data are the means ± SE. The M wave is the compound muscle action potential from sciatic-tibial innervated foot muscles. Comparisons were made using a one-way ANOVA with Bonferroni post hoc comparisons. *P < 0.05 (n = 5–7 per group). NAP, mixed caudal nerve action potential.

studied had diabetes of long duration (9 months) intermixed with a subset that recovered and were euglycemic between 6 and 9 months after diabetes initiation (all mice in the recovered group were originally diabetic until 6 months' post–STZ injection).

Electrophysiology. Electrophysiological recordings were made under anesthesia (Viking I; Nicolet, Madison, WI), as reported elsewhere in rats (9). Motor conduction velocity in sciatic-tibial fibers was assessed by stimulating at the sciatic notch and knee while recording the M wave (compound muscle action potential) from the tibial-innervated dorsal interossei foot muscles. Caudal conduction (sensory conduction velocity and mixed nerve action potentials) was recorded in the tail of mice by stimulating distally and recording proximally at fixed distances. Temperature near nerves was kept constant at 37°±1°C using a subdermal thermistor and heating lamp.

Morphometry. At the end point, tibial and sural nerves were removed and processed for epon embedding (10). Animals were subsequently killed with an overdose of sodium pentobarbital. Briefly, samples were fixed in 2.5% glutaraldehyde in 0.025 mol/l cacodylate buffer overnight, serially washed in 0.15 mol/l cacodylate buffer, postfixed in 2% osmium tetroxide in 0.12 mol/l

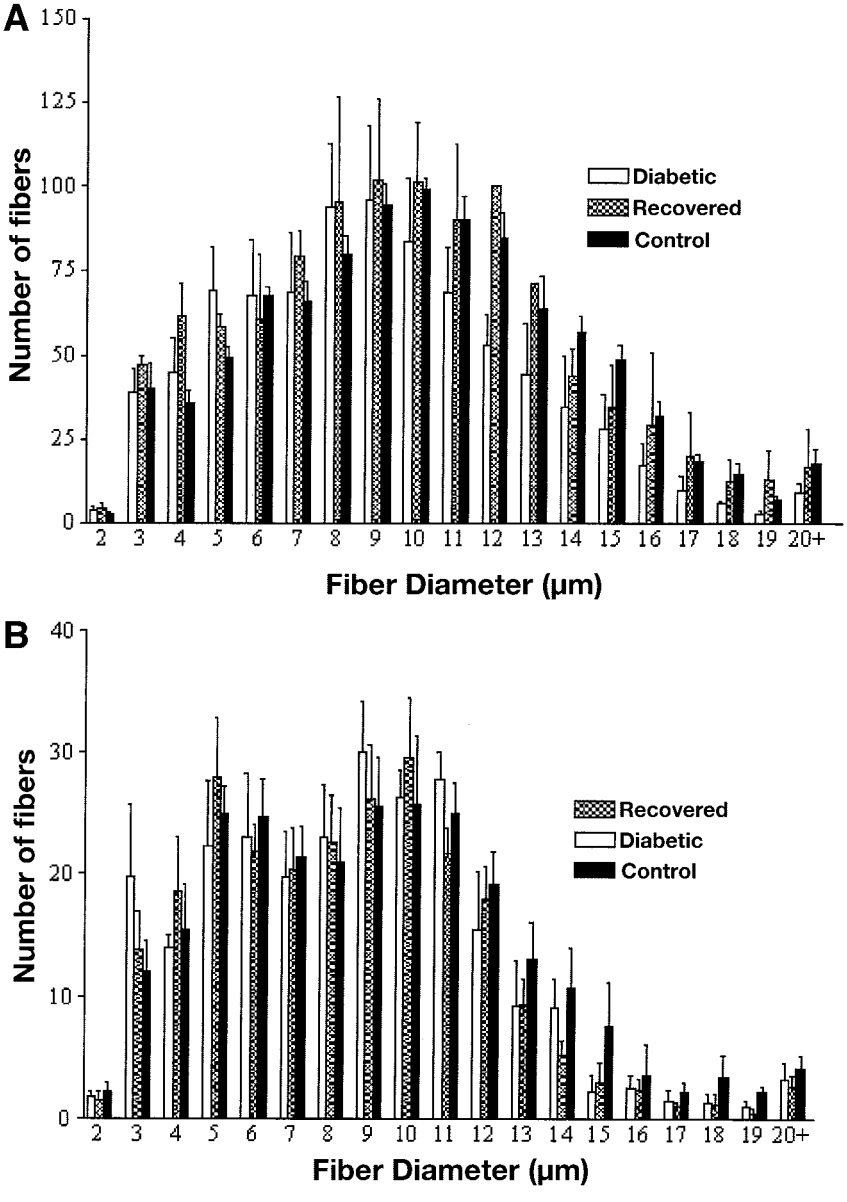

FIG. 1. *A*: Fiber size histogram of tibial fascicles from long-term mice (9-month diabetic, recovered, and control animals). There are fewer larger fibers (>9 μm) in diabetic animals, with a tendency for the recovered group to be in between diabetic and control numbers for each size category, especially larger fibers. A two-way ANOVA found significant differences (diabetic, nondiabetic, and recovered; P < 0.01) and diameter conditions only (P < 0.001), with no interaction effect between the two. Data are the means ± SE (n = 4 or 5 per group). *B*: Fiber size histogram of sural nerves from long-term mice. Myelinated fiber size histogram of the sural nerve (5 mm below sciatic trifurcation) in 9-month diabetic, recovered, and control animals. There tends to be fewer larger fibers (>13 μm) in diabetic and recovered animals compared with controls. A two-way ANOVA found significant differences (diabetic, nondiabetic, and recovered; P < 0.01) and diameter conditions (P < 0.001), with no interaction effect between the two. Data are the means ± SE (n = 4 or 5 per group).

TABLE 3
Morphologic properties of tibial fascicles from long-term mice

Property	Diabetic	Recovered	Nondiabetic
Fiber (n)	842 ± 183	1,048 ± 31	969 ± 41
Fiber density (n/mm^2)	18,550 ± 1,853	16,460 ± 1,243	15,730 ± 543
Density of small fibers (n/mm^2)	10,700 ± 1,310*	8,121 ± 1,114	7,092 ± 367
Density of large fibers (n/mm^2)	7,630 ± 452	8,338 ± 31	8,633 ± 212
Fiber diameter (μm)	8.6 ± 0.3*	9.4 ± 0.8	9.7 ± 0.1
Axon diameter (μm)	6.7 ± 0.2*	7.3 ± 0.7	7.6 ± 0.1
Myelin thickness (μm)	0.90 ± 0.07*	1.05 ± 0.05	1.08 ± 0.02
Fiber area (μm^2)	43.1 ± 2.6*	52.7 ± 4.6	57.0 ± 1.8
Axon area (μm^2)	27.9 ± 1.8*	33.3 ± 3.2	35.6 ± 1.4

Data are the means ± SE of 9-month diabetic, recovered, and nondiabetic mice (n = 4 or 5 per group). Comparisons were made between groups using a one-way ANOVA with Bonferroni post hoc t test. *$P < 0.05$.

cacodylate, dehydrated using a series of graded alcohols and propylene oxide, and embedded in epon. Transverse sections (1.0 μm thick) were cut with an ultramicrotome (Reichert, Vienna, Austria) using glass knives and were stained with toluidine blue. Morphologic examination of specimens used a JAVA-based image analysis program (Jandel Scientific) (11) obtained with a light microscope (Axioskope; Zeiss, North York, ON, Canada) and attached video camera (AVC-D7; Sony) interfaced with a computer. All counting was performed with the microscopist masked to the identity of the animal group.

Stereological counting. Dorsal root ganglia embedded in epon were serially cut (1 μm thick) on an ultramicrotome. The beginning of dorsal root ganglion tissue was considered to be the point at which at least 10 neuronal profiles were seen per transverse section (this became known as section A, or the reference section). A subsequent section was made 1 μm away from section A and served as a look-up section (section B). Neurons were counted as those with nuclear profiles that were visible in section A but not in section B. Neurons were differentiated from satellite and Schwann cells based on size and the presence of Nissl substance. The next pair of sections were processed in a similar manner at a predetermined distance interval, k (50 μm), away from the first set ($n + k$). Pairs of sections were then obtained for counting every 50 μm ($n + 2k$, $n + 3k$, $+ nk$), until only 10 neurons were seen once again (indicating the end of the dorsal root ganglion). Total neuronal number was then calculated based on the formula: N (number of neurons counted in all Axioskope sections) × k (distance interval). Sections were visualized (500×) and quantitated under a light microscope (Axioskope; Zeiss). Images were captured using a digital camera (Axiocam; Zeiss) and neuronal diameters measured using an interactive measurement module contained in an image analysis program (Axiovision 2.05; Zeiss). Only neurons with nuclear profiles were used to measure neuron diameters. All counting was performed with the microscopist masked to the identity of the experimental group.

Immunohistochemistry. Footpads were removed from the right plantar hind foot and fixed in Zamboni's fixative (2% paraformaldehyde in 0.1 mol/l phosphate buffer) overnight. The same anatomical footpads were used in each animal for comparison. Tissues were then washed 3 × 5 min in 0.1 mol/l PBS, followed by a 3 × 5-min DMSO wash, and finishing with a 3 × 5-min 0.1 mol/l PBS wash once again. Footpads were then cryoprotected overnight in 20% glycerol/0.1 mol/l PBS and subsequently frozen in optimum cutting temperature compound. Frozen sections were cut at 35 μm on a cryostat and thawed onto electrostatically charged slides (Superfrost Plus; VWR, Edmonton, Canada). For immunostaining, sections were subjected to antigen retrieval using a 20-min immersion in boiling sodium citrate (10 mmol/l) to expose the epitope. They were then lyophilized in 1% Triton X-100/PBS. After washes in 0.1 mol/l PBS (3 × 5 min), slides were incubated for 24 h in a humidified box at 4°C with rabbit anti–protein gene product 9.5 (1:800 dilution; Ultraclone, Cambridge, U.K.) diluted with 0.1 mol/l PBS, 1% NGS, and 0.3% Triton X-100. Slides were washed and incubated with Alexa 488 (1:500 dilution; Molecular Probes, Eugene, OR) anti-rabbit secondary antibody for 1 h at room temperature and mounted with Vectashield. Images were captured using an Olympus laser scanning confocal microscope equipped with epifluorescence. Z-stack images were obtained at 0.35-μm intervals through the section and combined (γ = 0.7) using Fluoview software (Olympus). Three fields per section and five sections per animal underwent quantitative analysis under a fluorescent microscope, and a mean value per mouse was calculated. Epidermal fibers were counted as those that extended from and above the dermal papillae. Fiber length was measured using an interactive measurement module (Axiovision 2.05; Zeiss) as the straight length the fiber extended into the epidermis irrespective of tortuosity. Sweat gland innervation was scored using a 5-point Likert scale (0 being no innervation, 5 being complete innervation). All counting and scoring was carried out with the microscopist blinded to the identity of each footpad.

Statistics. All data are presented as the means ± SE. Data were analyzed by a one-way ANOVA with Bonferroni corrected post hoc Student t test comparisons. For comparing diameter histograms (group versus diameter), a two-way ANOVA was used, primarily to assess the interaction effect. In all tests, statistical significance was set at $\alpha = 0.05$.

RESULTS

Electrophysiology. Long-term diabetic animals demonstrated features of hyperglycemia, including polydipsia, polyuria, and a decrease in activity. Whole–blood glucose measurements verified significant hyperglycemia beginning 1 week after STZ injection and persisting at 6 and 9 months postinjection. Recovered mice had elevated blood glucose levels at 1 week and 6 months, but by 9 months they had spontaneous recovery of islet function, with glycemia approaching the control range. Weights of diabetic

TABLE 4
Morphologic properties of the sural nerve in long-term mice

Property	Diabetic	Recovered	Nondiabetic
Fiber (n)	253 ± 5	247 ± 26	264 ± 43
Fiber density (n/mm^2)	17,080 ± 674	18,890 ± 1,549	18,050 ± 616
Density of small fibers (n/mm^2)	10,880 ± 1,596	11,880 ± 1,753	10,990 ± 942
Density of large fibers (n/mm^2)	6,866 ± 647	7,418 ± 346	7,658 ± 562
Fiber diameter (μm)	7.9 ± 0.2*	8.1 ± 0.4	8.6 ± 0.1
Axon diameter (μm)	6.7 ± 0.2	6.6 ± 0.3	7.0 ± 0.1
Myelin thickness (μm)	0.70 ± 0.00*	0.78 ± 0.37	0.80 ± 0.26
Fiber area (μm^2)	37.1 ± 3.2	36.4 ± 2.3	40.9 ± 0.8
Axon area (μm^2)	26.4 ± 2.0	24.4 ± 1.7	28.2 ± 0.4

Data are the means ± SE of 9-month diabetic, recovered, and nondiabetic mice. Comparisons were made between groups using a one-way ANOVA with Bonferroni post hoc t test. The sural nerve was sampled 5 mm distal to the sciatic trifurcation. *$P < 0.05$ (n = 4 or 5 per group).

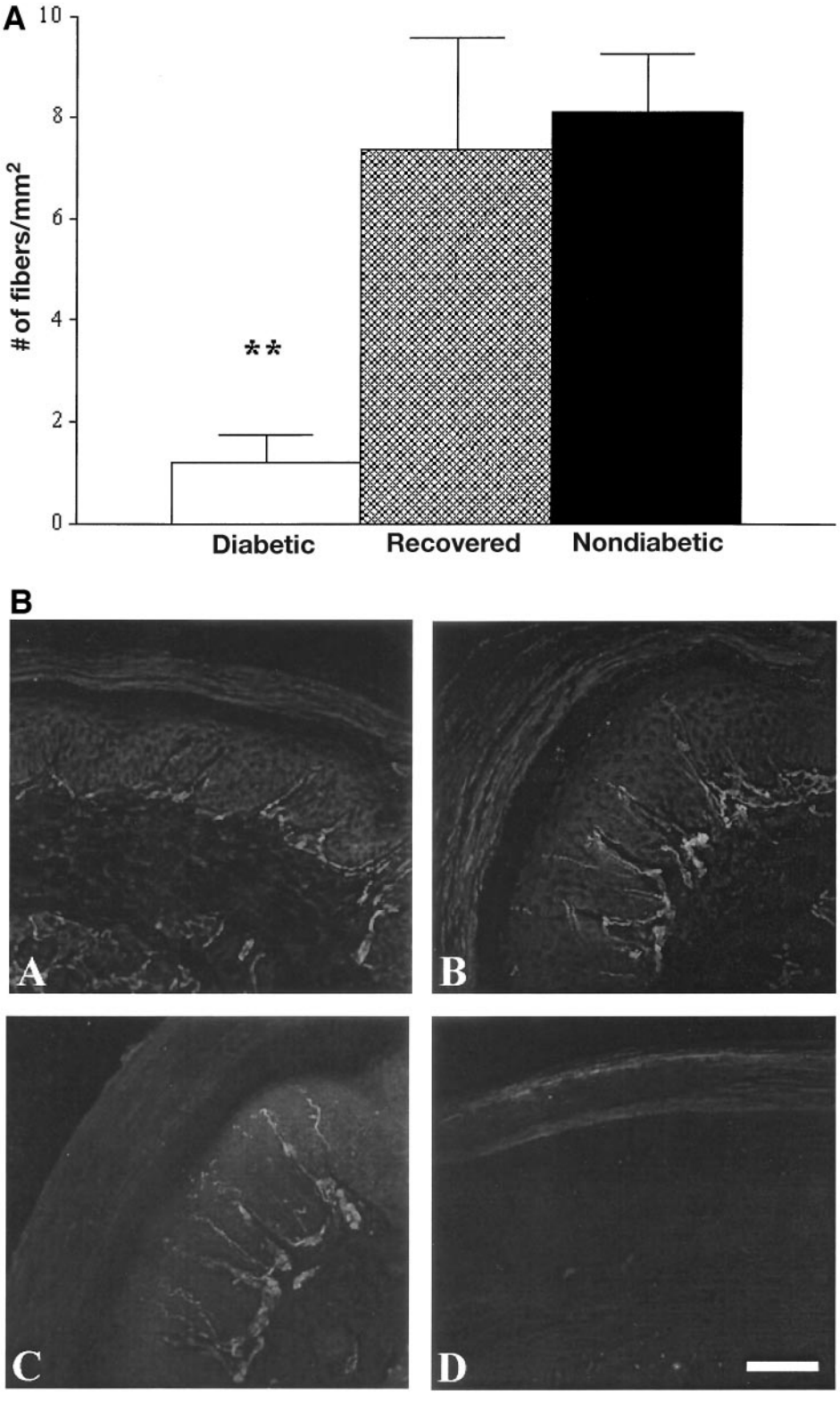

FIG. 2. ***A*****: Epidermal fiber density in footpads of long-term mice (9-month diabetic, recovered, and nondiabetic mice). Three microscope fields were counted per section, with five sections per animal used and averaged (each section yielded fit three or four fields). Data are the means ± SE. Nondiabetic and recovered groups had significantly higher epidermal fiber densities than diabetic groups. Groups were compared using a one-way ANOVA with Bonferroni post hoc Student's** ***t*** **test. *****P* **< 0.001.** ***B*****: Confocal micrographs of footpads from long-term mice stained with protein gene product 9.5. Panels show footpads from diabetic (A), recovered (B), nondiabetic (C), and negative control (D) mice. Diabetic footpads have significantly less protein gene product 9.5 immunoreactivity, indicating less epidermal fibers. The negative control consisted of the secondary antibody with omission of the primary. Magnification bar = 40 μm.**

and recovered mice were similar and significantly less than control mice by the end point ($P < 0.01$) (Table 1).

Diabetic mice had slowing of motor conduction velocity, reduced compound muscle action potential amplitudes (*M* waves), a trend (nonsignificant) toward sensory conduction velocity slowing, and reduced caudal nerve action potential amplitudes. In contrast, recovered mice did not demonstrate any abnormal electrophysiological measurements by the 9-month end point (Table 2). Indeed, there was a nonsignificant trend toward higher motor conduction velocity in recovered mice.

Axon numbers and structure. Myelinated fiber density and number in tibial fascicles, prominently populated by motor axons, were not altered by long-term diabetes. Mean fiber and axonal diameters and areas were smaller in diabetic mice ($P < 0.05$), but the recovered group had

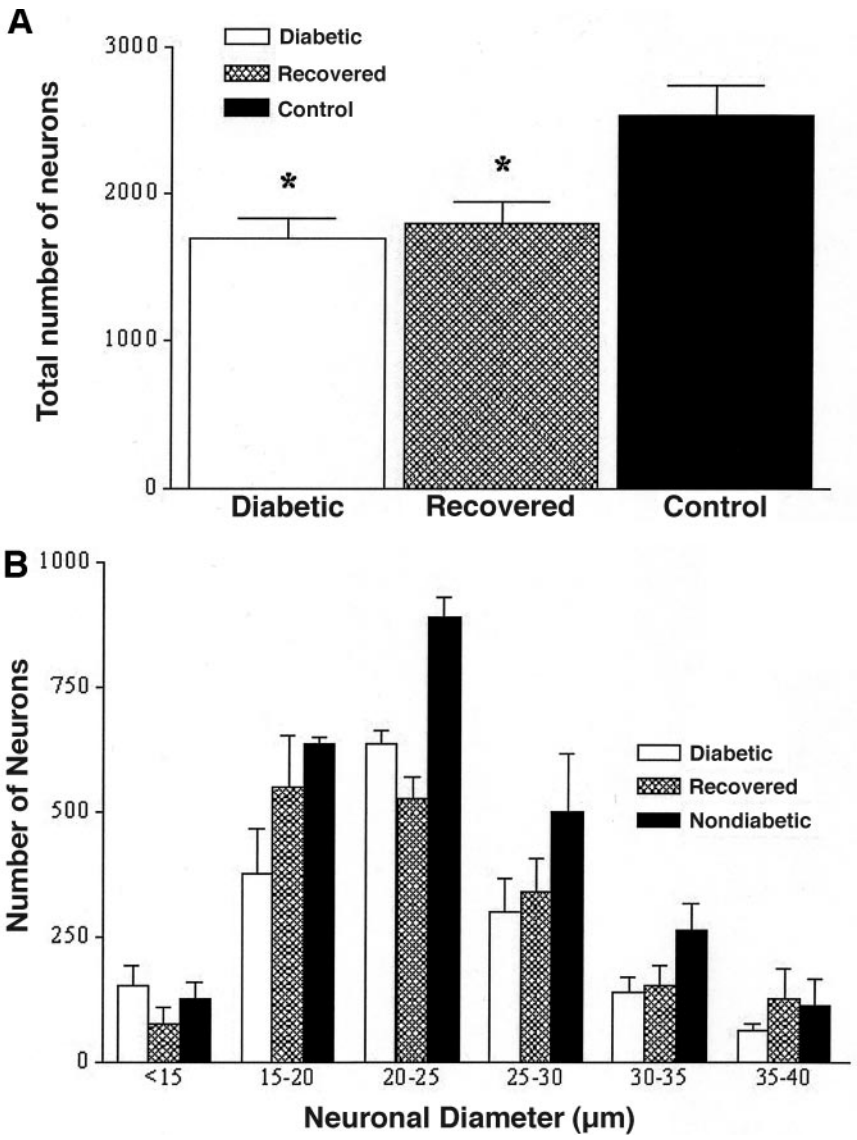

FIG. 3. ***A*****: Total number of neurons in L_5 dorsal root ganglia of long-term diabetic, recovered, and nondiabetic mice. Recovered mice are those that originally were diabetic but that reverted to euglycemia between 6 and 9 months after diabetes initiation. Data are the means ± SE. All three groups were compared using a one-way ANOVA with Bonferroni post hoc comparison. *$P < 0.05$. *B*: Diameter histogram of L_5 dorsal root ganglion neurons of long-term diabetic, recovered, and nondiabetic mice. Data are the means ± SE of each size. A two-way ANOVA was performed (treatment, $P < 0.001$; diameter, $P < 0.001$; interaction, not significant).**

near-normal calibers (Fig. 1*A*). Myelin in tibial fascicles was thinner in diabetic mice but not in recovered mice ($P < 0.05$) (Table 3). Diabetic sural nerves populated by sensory (and some autonomic) axons also had preserved fiber density and numbers. Mean fiber, but not axonal, diameter was reduced in both the diabetic and recovered groups ($P < 0.05$) (Fig. 1*B*) and was attributed to thinner myelin in the former ($P < 0.05$) (Table 4).

Epidermal nerve fiber innervation. Diabetic animals had significantly reduced numbers of epidermal fibers in plantar footpads ($P < 0.001$) (Fig. 2*A*). There was also dermal denervation with decreased sweat gland–associated axons as judged using a rating scale (diabetic: 1.3 ± 0.7; recovered: 3.8 ± 0.6; nondiabetic: 3.8 ± 0.5; $P < 0.05$; maximum score = 5). Recovered animals had epidermal fiber numbers similar to nondiabetic animals (Fig. 2*B*). Dermal and sweat gland innervation were also similar between recovered and nondiabetic groups. Recovered animals, however, did have longer epidermal fibers than either diabetic or nondiabetic animals (diabetic: 21.5 ± 1.5 μm; recovered: 25.0 ± 0.9 μm; nondiabetic: 21.9 ± 0.6 μm; $P < 0.05$).

Neuronal counting. Using the unbiased physical dissector stereological counting method, nondiabetic animals had a mean of 2,538 ± 200 neurons with a mean diameter of 23.6 ± 1.2 μm in the L_5 dorsal root ganglia. Diabetic animals had significantly fewer neurons compared with controls ($P < 0.05$). Mice with recovery also had fewer neurons ($P < 0.05$), with values similar to unrecovered diabetic animals (diabetic: 1,690 ± 143; recovered: 1,803 ± 145) (Fig. 3*A*). There was no difference in mean neuronal diameter among all three groups (diabetic: 23.4 ± 0.6 μm; recovered: 23.3 ± 0.6 μm) (Fig. 3*B*). Though not quantitated, neurons of diabetic and recovered mice appeared darker, with less nucleolar definition (Fig. 4).

DISCUSSION

The major findings of the present study were: *1*) long-term diabetic mice developed indexes of hyperglycemia with significant weight loss, similar to that of untreated humans; *2*) a significant number of previously hyperglycemic diabetic mice reverted to near-euglycemia, indicating spontaneous recovery from diabetes; *3*) long-term diabetic mice demonstrated electrophysiological abnormalities observed in human disease (i.e., reduced motor conduction velocity, decreases in amplitudes of *M* waves and nerve

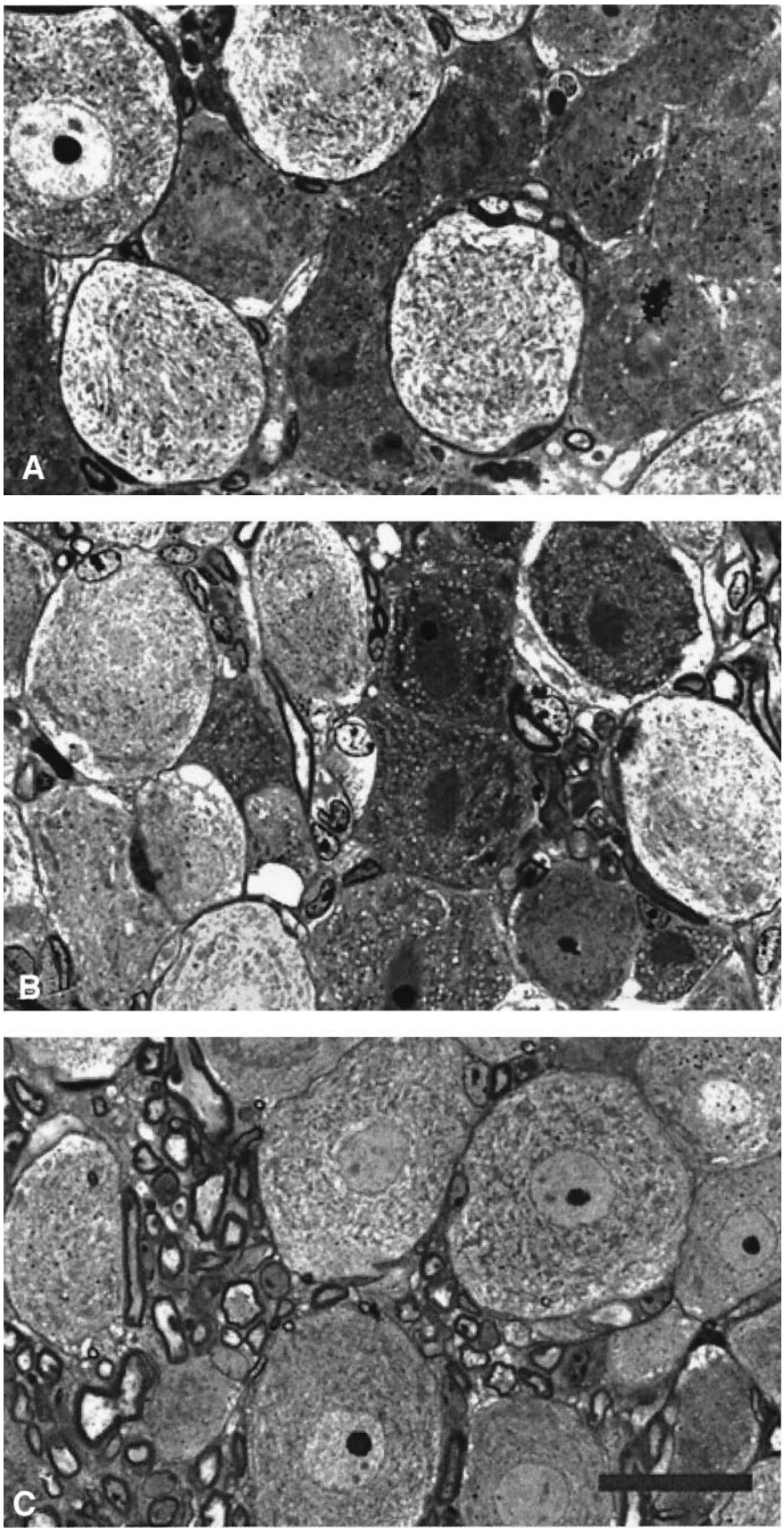

FIG. 4. Photomicrographs of dorsal root ganglion neurons from long-term mice. Panels show dorsal root ganglion neurons of 9-month diabetic (*A*), recovered (*B*), and nondiabetic (*C*) mice. Diabetic and recovered animals had fewer neurons. A subset of the remaining population, though not quantitated, appeared darker and had less nucleolar definition. Scale bar = 20 μm.

action potentials; electrophysiological abnormalities disappeared in recovered mice); *4*) other structural abnormalities of the long-term murine model of diabetes closely modeled human disease (i.e., axon atrophy, myelin thinning, loss of epidermal axons, loss of sweat gland innervation, and sensory neuron loss); and *5*) recovered mice

had recovery of axonal structural abnormalities but no recovery of lost neurons.

Our long-term diabetic mouse model helps with some difficulties that have arisen in studies of STZ-induced diabetic rat models. STZ-induced diabetic mice reportedly develop pancreatic lesions similar to patients with type 1 diabetes. Cytokines or reactive radicals released during T-cell–mediated pancreatic islet inflammation may involve activation of poly(ADP-ribose) polymerase or inducible nitric oxide synthase (12–14), with selective targeting of GLUT2 by STZ (15,16). Our mice survived long periods of diabetes without exogenous insulin administration. Because STZ-induced diabetic mice do not progress into ketoacidosis (unlike NOD mice), it is likely that the pancreas continues to produce small amounts of insulin. An unexpected finding, however, was the reversion to near-euglycemia of a subset of these chronically diabetic animals, as also reported by Li et al. (17), Hartman et al. (18), and George et al. (19). All of the animals in the recovered group had diabetes for at least 6 months, with a critical reversion point thereafter. Given the loss of sensory neurons, it is clear that neuropathy had developed before recovery. In other cohorts of mice, identically studied, electrophysiological abnormalities are well established by 3–4 months (well before the 6-month reversion time point in this study). It is also important to note that despite dramatically improved glycemia in the recovered mice, mean plasma glucose persisted somewhat above control values. Although STZ-induced diabetic rat models similarly develop significant slowing of motor and sensory conduction velocity (20,21), they do not later exhibit the loss of *M* waves or nerve action potentials or the myelin thinning that are observed in humans.

In diabetic neuropathy, a sequence of reversible, largely electrophysiological abnormalities likely involves metabolic derangements, such as polyol accumulation (22–26), decreased Na-K-ATPase activity, and intra-axonal sodium accumulation leading to slowed conduction (24,27). Sensory neurons may be more susceptible to irreversible structural damage. Degeneration of both myelinated and unmyelinated fibers particularly in sural sensory nerves are often noted in nerve biopsies from diabetic patients (28). The very distal loss of fibers in sural nerves also seen in the murine model (29) may support the concept that defects in growth factor synthesis, uptake, or signaling contribute to diabetic neuropathy (30–33). Growth factor deficiency may also be compounded by slowed retrograde axonal transport, limiting delivery of growth factors to proximal neurons (34–36). Akkina et al. (37) identified early involvement of nonpeptidergic unmyelinated afferents in STZ-induced diabetic mice that were rescued by trophic therapy. Our finding of epidermal nerve fiber loss is a striking parallel to human disease. Axonal degeneration in human diabetic neuropathy is often also associated with attempted regeneration (38,39). We did not detect evidence of regenerative clusters or sprouts in diabetic mice.

In our long-term mice, there was substantial loss in the number of sensory neurons in diabetic and recovered animals. Russell et al. (40) have argued for an aggressive circle of apoptosis in diabetic rat dorsal root ganglion neurons, secondary to mitochondrial dysfunction. This level of loss, however, has not been observed in actual rat diabetic models. Kishi et al. (41) and Zochodne et al. (5) failed to demonstrate sensory neuron loss in long-term diabetic rats. Later events in diabetic neuropathy may also center around impaired axonal transport of neurofilaments or other cytoskeletal structures (42). Limited cytoskeletal support by perikarya may result in flawed axons or axons that are incapable of dynamic restructuring (because of rapid glycosylation of proteins). Excessive production of free radicals in diabetes or oxidative stress may generate "all or none" irreversible damage.

Had recovery been associated with replenishment of sensory neuron populations, this would have been a surprising finding, given the long-term evidence that perikaryal loss is essentially irretrievable. The robust collateral reinnervation of the skin arising in recovered diabetic mice is of considerable interest. For example, it may be that preventing some perikaryal loss is impossible in diabetic patients. The knowledge that remaining neurons may be capable of reinnervating some denervated target tissues if β-function recovers may be important to exploit. Although such striking collateral reinnervation may simply arise because neurons are no longer exposed to hyperglycemia, restored insulin signaling may be more relevant. Insulin receptor expression appears to rise in diabetes, and direct administration of insulin to sensory neurons appears capable of restoring neuron function independently of glycemic levels (43–45). Insulin support may repair neuronal function by reversing deficits in mitochondrial depolarization (46). Insulin also appears to offer significant support to regenerative sprouting (47,48) and could support collateral sprouting through synergistic actions with neurotrophic growth factors that provide such support (49–51).

Our results demonstrate that long-term experimental murine diabetes models human diabetic neuropathy in a number of important aspects. It seems evident, from this model, that neuropathy is not a single continuous process, but rather it represents interchanging activities differentially involving in sensory and motor components. Spontaneous recovery from diabetes rendering near-euglycemia allows many features of neuropathy to recover. Importantly, however, it cannot resurrect sensory neurons once lost. Clinical approaches to reconstitute islet function may also need to protect the sensory neuron directly.

REFERENCES

1. Amos AF, McCarty DJ, Zimmet P: The rising global burden of diabetes and its complications: estimates and projections to the year 2010. *Diabet Med* 14 (Suppl. 5):S1–S85, 1997
2. King H, Aubert RE, Herman WH: Global burden of diabetes, 1995–2025: prevalence, numerical estimates, and projections. *Diabetes Care* 21:1414–1431, 1998
3. Shapiro AM, Lakey JR, Ryan EA, Korbutt GS, Toth E, Warnock GL, Kneteman NM, Rajotte RV: Islet transplantation in seven patients with type 1 diabetes mellitus using a glucocorticoid-free immunosuppressive regimen. *N Engl J Med* 343:230–238, 2000
4. Dyck PJ, Kratz KM, Lehman KA, Karnes JL, Melton LJ 3rd, O'Brien PC, Litchy WJ, Windebank AJ, Smith BE, Low PA, et al.: The Rochester Diabetic Neuropathy Study: design, criteria for types of neuropathy, selection bias, and reproducibility of neuropathic tests. *Neurology* 41:799–807, 1991
5. Zochodne DW, Verge VMK, Cheng C, Sun H, Johnston J: Does diabetes target ganglion neurons? Progressive sensory neuron involvement in long term experimental diabetes. *Brain* 124:2319–2334, 2001
6. Boulton AJM: Foot problems in patients with diabetes mellitus. In *Textbook of Diabetes*. Pickup J, Williams G, Eds. Oxford, U.K., Blackwell Science, 1997, p. 58.1–58.20

7. Brown MJ, Asbury AK: Diabetic neuropathy. *Ann Neurol* 15:2–12, 1984
8. Zochodne DW, Murray MM, van der Sloot P, Riopelle RJ: Distal tibial mononeuropathy in diabetic and nondiabetic rats reared on wire cages: an experimental entrapment neuropathy. *Brain Res* 698:130–136, 1995
9. Zochodne DW, Ho LT: The influence of indomethacin and guanethidine on experimental streptozotocin diabetic neuropathy. *Can J Neurol Sci* 19: 433–441, 1992
10. Zochodne DW, Misra M, Cheng C, Sun H: Inhibition of nitric oxide synthase enhances peripheral nerve regeneration in mice. *Neurosci Lett* 228:71–74, 1997
11. Auer RN: Automated nerve fibre size and myelin sheath measurement using microcomputer-based digital image analysis: theory, method and results. *J Neurosci Methods* 51:229–238, 1994
12. Burkart V, Wang ZQ, Radons J, Heller B, Herceg Z, Stingl L, Wagner EF, Kolb H: Mice lacking the poly(ADP-ribose) polymerase gene are resistant to pancreatic beta-cell destruction and diabetes development induced by streptozocin. *Nat Med* 5:314–319, 1999
13. Mabley JG, Suarez-Pinzon WL, Hasko G, Salzman AL, Rabinovitch A, Kun E, Szabo C: Inhibition of poly (ADP-ribose) synthetase by gene disruption or inhibition with 5-iodo-6-amino-1,2-benzopyrone protects mice from multiple-low-dose-streptozotocin-induced diabetes. *Br J Pharmacol* 133: 909–919, 2001
14. Flodstrom M, Tyrberg B, Eizirik DL, Sandler S: Reduced sensitivity of inducible nitric oxide synthase-deficient mice to multiple low-dose streptozotocin-induced diabetes. *Diabetes* 48:706–713, 1999
15. Hosokawa M, Dolci W, Thorens B: Differential sensitivity of GLUT1- and GLUT2-expressing beta cells to streptozotocin. *Biochem Biophys Res Commun* 289:1114–1117, 2001
16. Wang Z, Gleichmann H: GLUT2 in pancreatic islets: crucial target molecule in diabetes induced with multiple low doses of streptozotocin in mice. *Diabetes* 47:50–56, 1998
17. Li Z, Karlsson FA, Sandler S: Islet loss and alpha cell expansion in type 1 diabetes induced by multiple low-dose streptozotocin administration in mice. *J Endocrinol* 165:93–99, 2000
18. Hartmann K, Besch W, Zuhlke H: Spontaneous recovery of streptozotocin diabetes in mice. *Exp Clin Endocrinol* 93:225–230, 1989
19. George M, Ayuso E, Casellas A, Costa C, Devedjian JC, Bosch F: β cell expression of IGF-I leads to recovery from type 1 diabetes. *J Clin Invest* 109:1153–1163, 2002
20. Kalichman MW, Dines KC, Bobik M, Mizisin AP: Nerve conduction velocity, laser Doppler flow, and axonal caliber in galactose and streptozotocin diabetes. *Brain Res* 810:130–137, 1998
21. Cameron NE, Cotter MA, Jack AM, Basso MD, Hohman TC: Protein kinase C effects on nerve function, perfusion, Na(+), K(+)-ATPase activity and glutathione content in diabetic rats. *Diabetologia* 42:1120–1130, 1999
22. Field RA: Altered nerve metabolism in diabetes. *Diabetes* 15:696–698, 1966
23. Gabbay KH, Merola LO, Field RA: Sorbitol pathway: presence in nerve and cord with substrate accumulation in diabetes. *Science* 151:209–210, 1966
24. Gould RM: Inositol lipid synthesis localized in axons unmyelinated fibers of peripheral nerve. *Brain Res* 117:168–174, 1976
25. Greene DA, Sima AA, Stevens MJ, Feldman EL, Lattimer SA: Complications: neuropathy, pathogenetic considerations. *Diabetes Care* 15:1902–1925, 1992
26. Greene DA, Lattimer SA, Sima AA: Sorbitol, phosphoinositides, and sodium-potassium-ATPase in the pathogenesis of diabetic complications. *N Engl J Med* 316:599–606, 1987
27. Mandersloot JG, Roelofsen B, de Gier J: Phosphatidylinositol as the endogenous activator of the (Na+ + K+)-ATPase in microsomes of rabbit kidney. *Biochim Biophys Acta* 508:478–485, 1978
28. Dyck PJ, Lais A, Karnes JL, O'Brien P, Rizza R: Fiber loss is primary and multifocal in sural nerves in diabetic polyneuropathy. *Ann Neurol* 19:425–439, 1986
29. Kennedy JM, Zochodne DW: The regenerative deficit of peripheral nerves in experimental diabetes: its extent, timing and possible mechanisms. *Brain* 123:2118–2129, 2000
30. Faradji V, Sotelo J: Low serum levels of nerve growth factor in diabetic neuropathy. *Acta Neurol Scand* 81:402–406, 1990
31. Hellweg R, Hartung H-D: Endogenous levels of nerve growth factor (NGF) are altered in experimental diabetes mellitus: a possible role for NGF in the pathogenesis of diabetic neuropathy. *J Neurosci Res* 26:258–267, 1990
32. Ishii DN: Implication of insulin-like growth factors in the pathogenesis of diabetic neuropathy. *Brain Res Brain Res Rev* 20:47–67, 1995
33. Zhuang HX, Wuarin L, Fei ZJ, Ishii DN: Insulin-like growth factor (IGF) gene expression is reduced in neural tissues and liver from rats with non-insulin-dependent diabetes mellitus, and IGF treatment ameliorates diabetic neuropathy. *J Pharmacol Exp Ther* 283:366–374, 1997
34. Jakobsen J, Brimijoin S, Skau K, Sidenius P, Wells D: Retrograde axonal transport of transmitter enzymes, fucose-labeled protein, and nerve growth factor in streptozotocin-diabetic rats. *Diabetes* 30:797–803, 1981
35. Mayer JH, Tomlinson DR: Axonal transport of cholinergic transmitter enzymes in vagus and sciatic nerves of rats with acute experimental diabetes mellitus; correlation with motor nerve conduction velocity and effects of insulin. *Neuroscience* 9:951–957, 1983
36. Larsen JR, Sidenius P: Slow axonal transport of structural polypeptides in rat, early changes in streptozocin diabetes, and effect of insulin treatment. *J Neurochem* 52:390–401, 1989
37. Akkina SK, Patterson CL, Wright DE: GDNF rescues nonpeptidergic unmyelinated primary afferents in streptozotocin-treated diabetic mice. *Exp Neurol* 167:173–182, 2001
38. Bradley JL, Thomas PK, King RHM, Muddle JR, Ward JD, Tesfaye S, Boulton AJM, Tsigos C, Young RJ: Myelinated nerve fibre regeneration in diabetic sensory polyneuropathy: correlation with type of diabetes. *Acta Neuropathol* 90:403–410, 1995
39. Dyck PJ, Giannini C: Pathologic alterations in the diabetic neuropathies of humans: a review. *J Neuropathol Exp Neurol* 55:1181–1193, 1996
40. Russell JW, Sullivan KA, Windebank AJ, Herrmann DN, Feldman EL: Neurons undergo apoptosis in animal and cell culture models of diabetes. *Neurobiol Dis* 6:347–363, 1999
41. Kishi M, Tanabe J, Schmelzer JD, Low PA: Morphometry of dorsal root ganglion in chronic experimental diabetic neuropathy. *Diabetes* 51:819–824, 2002
42. Bomers K, Braendgaard H, Flyvbjerg A, Sidenius P: Redistribution of axoplasm in the motor root in experimental diabetes. *Acta Neuropathol (Berl)* 92:98–101, 1996
43. Sugimoto K, Murakawa Y, Sima AA: Expression and localization of insulin receptor in rat dorsal root ganglion and spinal cord. *J Peripher Nerv Syst* 7:44–53, 2002
44. Brussee V, Cunningham FA, Zochodne DW: Direct insulin signaling of neurons reverses diabetic neuropathy. *Diabetes* 53:1824–1830, 2004
45. Singhal A, Cheng C, Sun H, Zochodne DW: Near nerve local insulin prevents conduction slowing in experimental diabetes. *Brain Res* 763:209–214, 1997
46. Huang TJ, Price SA, Chilton L, Calcutt NA, Tomlinson DR, Verkhratsky A, Fernyhough P: Insulin prevents depolarization of the mitochondrial inner membrane in sensory neurons of type 1 diabetic rats in the presence of sustained hyperglycemia. *Diabetes* 52:2129–2136, 2003
47. Xu QG, Li XQ, Kotecha SA, Cheng C, Sun HS, Zochodne DW: Insulin as an in vivo growth factor. *Exp Neurol* 188:43–51, 2004
48. Zochodne DW, Brussee V, McDonald D, Toth C: Differentiating the impact of peripheral and central delivery of insulin on sensory axon regeneration (Abstract). *Soc Neurosci Abs* 413:12, 2003
49. Diamond J, Gloster A, Kitchener P: Regulation of the sensory innervation of skin: trophic control of collateral sprouting. In *Sensory Neurons: Diversity, Development and Plasticity*. Scott SA, Ed. Oxford, U.K., Oxford University Press, 1992, p. 309–332
50. Diamond J, Holmes M, Coughlin M: Endogenous NGF and nerve impulses regulate the collateral sprouting of sensory axons in the skin of the adult rat. *J Neurosci* 12:1454–1466, 1992
51. Sayers NM, Beswick LJ, Middlemas A, Calcutt NA, Mizisin AP, Tomlinson DR, Fernyhough P: Neurotrophin-3 prevents the proximal accumulation of neurofilament proteins in sensory neurons of streptozocin-induced diabetic rats. *Diabetes* 52:2372–2380, 2003